

A HIGH-Q LENGTH-EXTENSIONAL BULK-MODE MASS SENSOR WITH ANNEXED SENSING PLATFORMS

Zhili Hao, Reza Abdolvand, and Farrokh Ayazi

Integrated MEMS Laboratory, School of Electrical and Computer Engineering,
Georgia Institute of Technology, 777 Atlantic Drive, Atlanta, GA 30332-0250, USA

ABSTRACT

This paper presents a length-extensional bulk-mode mass sensor with annexed sensing platforms and on-chip integrated capacitive transducers. The utilization of the bulk-mode vibrations of a resonant microstructure enables higher mass sensitivity at the micro-scale and high quality factor (Q) in air. Besides overcoming technical issues inherent with cantilever-based mass sensors, the annexed sensing platforms cover a large range of mass sensitivity within a single sensor-array chip. The measured highest mass sensitivity of this device is 215Hz/pg operating at 13MHz with a $Q\sim 4,000$ in air.

1. INTRODUCTION

Micro/nano-cantilever resonators coated with selective binding layers are of great interest for detecting chemical and/or biological species [1]. Although cantilever-based mass sensors have demonstrated attogram (in vacuum) [1] and femtogram (in air) mass detection [2], their complicated assembly for photothermal actuation and optical readout [1], and low quality factor (Q) in air make them less suitable for real-world detection using microsystem. Especially, a higher Q in a resonant mass sensor is desirable in that it translates to a higher signal-to-noise ratio and a lower minimum detectable mass [3].

There are some technical issues inherent with cantilever-based mass sensors. For instance, resonant frequency shift should ideally be caused by the absorbed mass only. However, the adsorption process introduces stiffness variation of a cantilever [4], complicating the interpretation of experimental results. Since the resonant vibration amplitude along the length of a cantilever is different, non-uniform adsorption of species will further introduce error in experimental measurement.

To overcome the above-mentioned technical issues of a cantilever-based mass sensor, this work presents the concept of a bulk-mode mass sensor and the experimental results for such devices. By using the length-extensional bulk-mode vibrations of a resonant microstructure, this device offers advantages of 1) higher mass sensitivity at the micro-scale; 2) high-quality factor (Q) in air; 3) on-chip integration with capacitive or piezoelectric transducers; and 4)

compatibility with sensor array configuration for field applications.

2. CONCEPT GENERATION

Working Principle

As shown in Figure 1, a length-extensional bulk-mode mass sensor consists of a central block and two sensing platforms annexed to the block through separation beams. The whole resonant microstructure is suspended from the substrate by two support beams. A selective binding layer is coated on top of the two annexed sensing platforms. This device operates in its length-extensional bulk-mode, as shown in Figure 2. By measuring resonant frequency shift Δf , the mass sensor monitors mass loading Δm due to species adsorption.

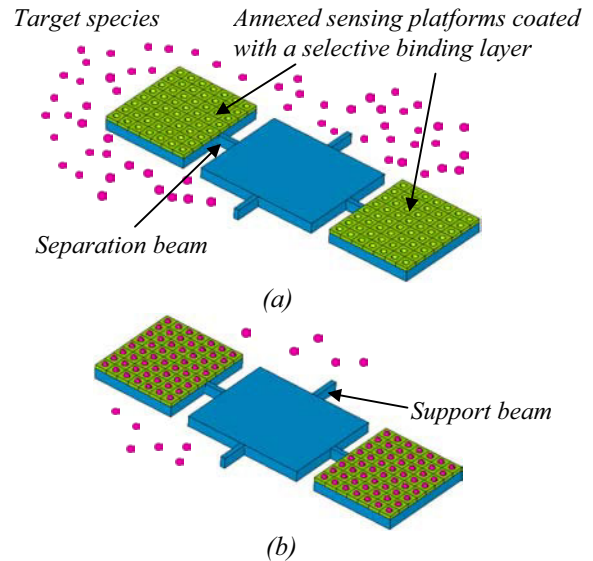


Figure 1. Working principle of a bulk-mode mass sensor (a) before absorbing target species and (b) after absorbing target species

Annexed Sensing Platforms

The utilization of the annexed platforms for species adsorption provides unprecedented performance improvement. As illustrated in Figure 2, by introducing slim separation beams into the resonant structure, the deformation in the annexed sensing platforms are greatly alleviated, resulting in a translational-dominant motion. Therefore, species absorption on the platforms

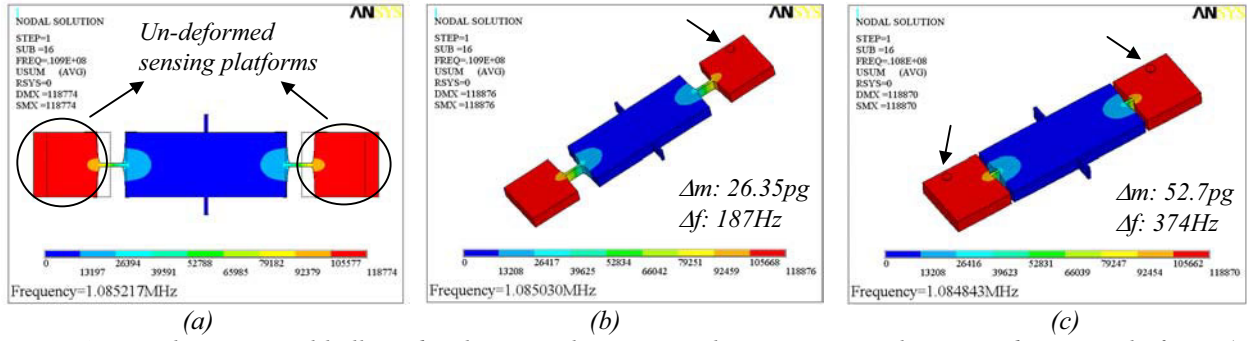


Figure 2. Length-extensional bulk-mode vibrations showing translation motion in the annexed sensing platforms (a) mode shape without mass loading; (b) mode shape with a loaded mass of 26.35pg (on one platform); and (c) mode shape with a loaded mass of 52.7pg (on both platforms)

has much less effect on the equivalent stiffness ($\Delta k \sim 0$), and mass loading becomes the main mechanism for shift in resonant frequency. This is verified by numerical simulation (Figure 2), where the frequency shift is proportional to the loaded mass.

Due to the near-uniform motion of the platforms (in areas sufficiently away from the separation beam), the adsorbed species across the platforms has the same contribution to the equivalent mass, and hence non-uniform adsorption does not complicate the interpretation of experimental results. Also, since the annexed platforms experience the maximum vibration amplitude, the adsorbed species cause the *largest* shift in resonant frequency of the device.

On-chip Transducers

This mass sensor can be operated with on-chip capacitive (Figure 3) or piezoelectric (Figure 4) transducers with a two-port configuration. This work employs capacitive transducers to demonstrate the proof of concept. The main geometrical design parameters are illustrated in Figure 3. The resonant structure is connected to a DC polarization voltage (V_p). An ac voltage (v_d) is applied to the drive electrode, while a sensing current (i_s) is detected from the sense electrode.

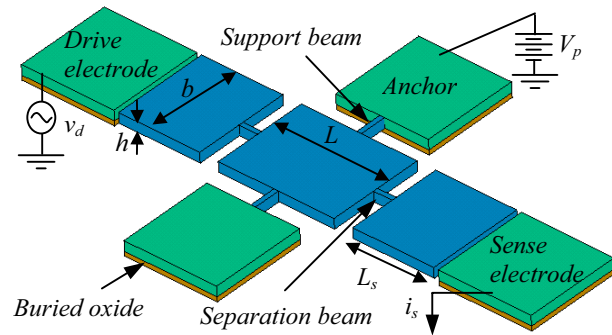


Figure 3. Two-port configuration of a length-extensional mass sensor with capacitive transducers

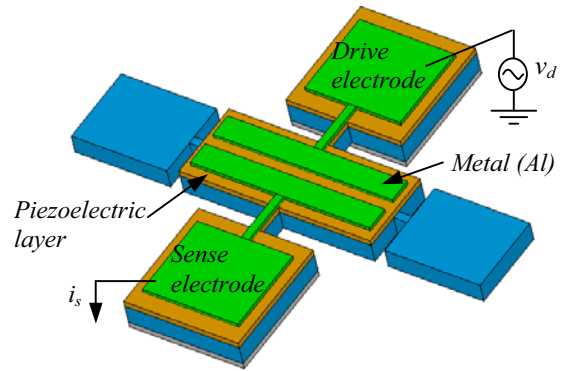


Figure 4. Two-port configuration of a length-extensional mass sensor with piezoelectric transducers

Figures of Merit

The mass sensitivity (S_m) of this device can be expressed as [3]:

$$S_m = \frac{\Delta f}{\Delta m} = \frac{f_0}{4\rho \cdot b \cdot h \cdot L_s \cdot \lambda_{eff}} \quad (1)$$

where ρ is the density of the resonant structure's material; f_0 is the initial resonant frequency before adsorption of species; and $\lambda_{eff} > 1$ is a geometrical coefficient of the resonant structure. According to Equation (1), by varying the in-plane length (L_s) of annexed sensing platforms, this design can cover a large range of mass sensitivity within one single sensor-array chip.

The theoretical minimum detectable mass (Δm_{min}) of this device is expressed as [3]:

$$\Delta m_{min} = \frac{\sqrt{4k_b \cdot T \cdot B}}{x} \sqrt{\frac{2\rho \cdot b \cdot h \cdot L_s \cdot \lambda_{eff}}{Q \cdot (2\pi)^3 \cdot f_0^3}} \quad (2)$$

where k_b and T denote the Boltzman Constant and the environment temperature, respective; B is Bandwidth; and x is the vibration amplitude.

3. EXPERIMENTAL VERIFICATION

We have fabricated such devices on a $4.3\mu\text{m}$ -thick SOI wafer using one single mask fabrication process [5]. Figure 5 shows a SEM picture of this bulk-mode mass sensor with the capacitive gaps in the range of 600nm .

To evaluate the performance of this mass sensor, known amount of nanoparticles (Cerium from nGimat Co., diameter $<20\text{nm}$) are placed on its annexed platforms, using a very fine probe tip (radius= $2.5\mu\text{m}$) under a microscope. This has the same effect as mass loading due to species adsorption. Figure 6 shows SEM pictures of the mass sensors with clusters of nanoparticles loaded on the sensing platforms. To measure the mass sensitivity of this device, the resonant frequencies of a device are measured both before and after mass loading, as illustrated in Figure 7. The resonant frequency decreases due to a mass load of $\sim 1\text{pg}$.

We have successfully measured the resonant frequency shifts and Q at various bias voltages of the devices ($L=50\mu\text{m}$, $b=40\mu\text{m}$, and $v_d=1.25\text{V}$) with different sensing platform lengths. Figures 8 and 9 show the measured frequency shifts at various bias voltages and the corresponding Q of the devices with $L_s=40\mu\text{m}$ and $L_s=45\mu\text{m}$, respectively. The measured Q ranges

from $3,800$ to $4,400$ in air, clearly showing that mass loading does not affect the Q values. The measured loaded mass is consistent at different bias voltages for these devices and is in good agreement with theoretical calculation from Equation (1).

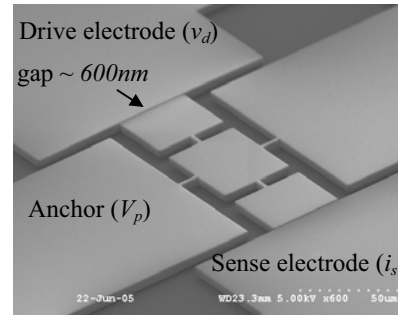


Figure 5. A SEM picture of the fabricated mass sensor

The performance of the mass sensors (Figure 5(b), 7, and 8) is summarized in Table 1. By varying the sensing platform length from $35\mu\text{m}$ to $45\mu\text{m}$, the mass sensitivity can be tuned from 215Hz/pg to 151Hz/pg . Both the mass sensitivity and the quality factor of this device are much larger than the corresponding values (66Hz/pg and

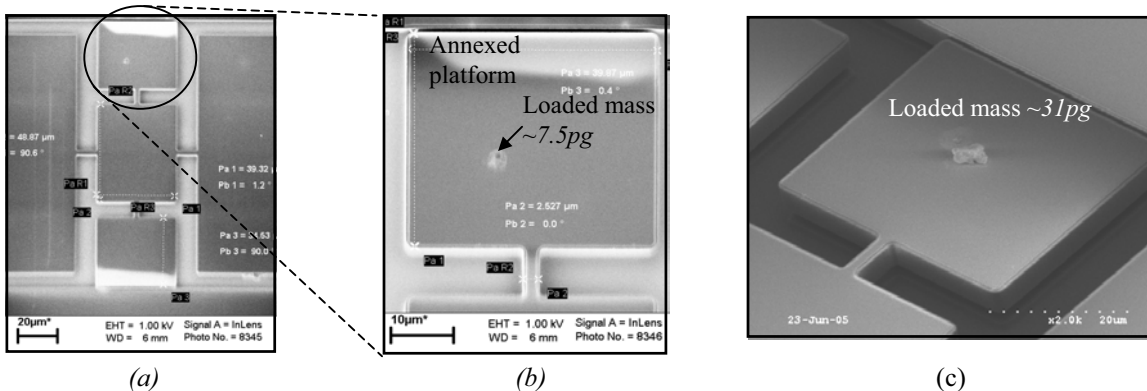


Figure 6. SEM pictures of mass sensors with loaded mass (a) Top view with mass loading; (b) Loaded mass $\sim 7.5\text{pg}$; and (c) Loaded mass $\sim 31\text{pg}$

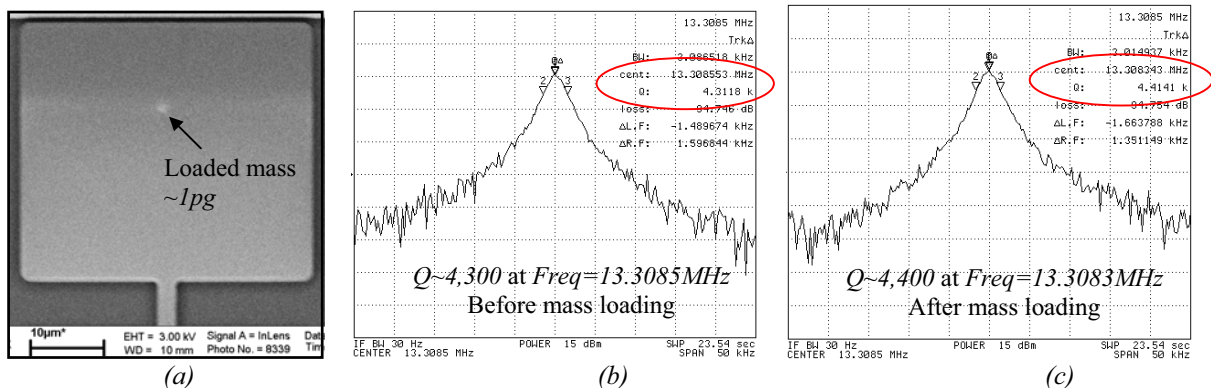


Figure 7. Resonant frequency and Q measured in air for a mass sensor ($L=50\mu\text{m}$ and $L_s=35\mu\text{m}$) with loaded mass $\sim 1\text{pg}$ (a) SEM picture; (b) $V_p=125\text{V}$, before mass loading; and (c) $V_p=125\text{V}$, after mass loading

$Q < 100$ at $freq < 100kHz$) of a sub-micron thick cantilever [6]. Based on Equation (2), the theoretical Δm_{min} of this device in air is comparable to that of a nano-cantilever in vacuum [1].

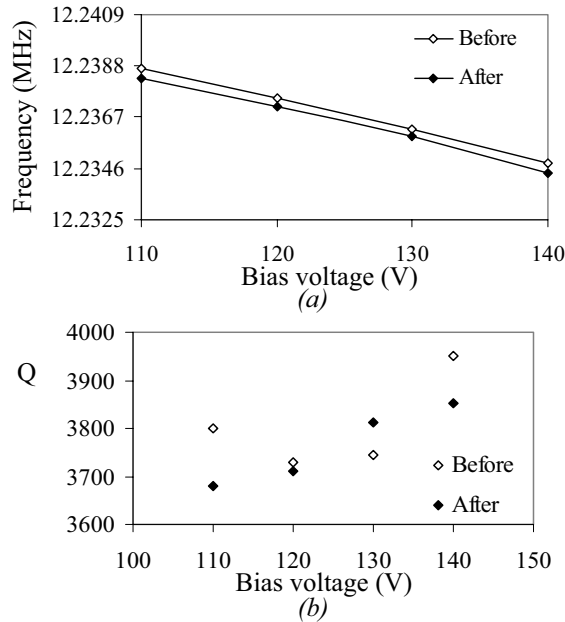


Figure 8. Performance measured in air before and after mass loading ($\sim 2pg$) for a mass sensor ($L_s=40\mu m$) (a) measured resonant frequency and (b) measured Q

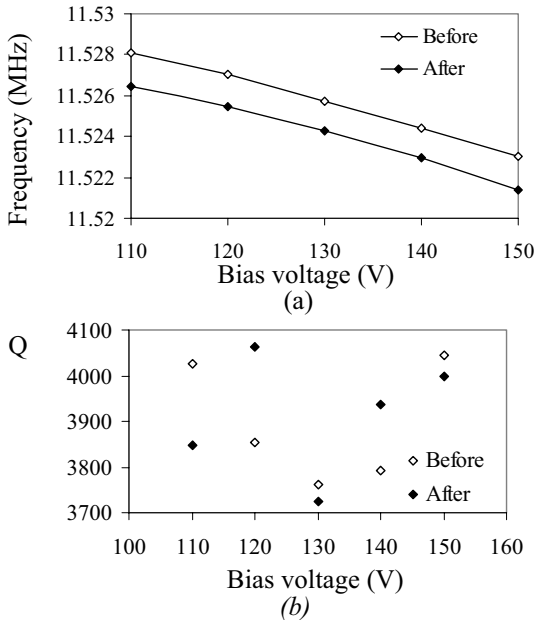


Figure 9. Performance measured in air before and after mass loading ($\sim 10pg$) for a mass sensor ($L_s=45\mu m$) (a) measured resonant frequency and (b) measured Q

4. CONCLUSION

A length-extensional bulk-mode mass sensor has been developed with high- Q and integrated transducers,

showing better performance in air and compatibility with sensor array configuration. To lower the bias voltage, HARPSS-on-SOI process can be used to reduce the capacitive gaps ($< 200nm$) [7]. Alternatively, piezoelectric transduction can be used on the central block of the device [8], providing more flexibility for various detection environments. This device can be further integrated into oscillator circuits for practical detection at the micro-scale.

Table 1. Performance summary of the length-extensional mass sensor

Sensing platform length (μm)	35	40	45
Resonant frequency (MHz)	13.392	12.245	11.534
Drive and sense gap (nm)	680	560	570
Quality factor (Q)	4400	3800	4000
Vibration amplitude (nm)	12	12	13
Mass sensitivity (Hz/pg)	215	177	151
Minimum detectable mass (attogram)	1.17	1.52	1.57

ACKNOWLEDGMENT

This work is supported by the NSF Packaging Research Center at Georgia Tech.

REFERENCES

- [1] B. Llic, H. G. Craighead, S. Krylov, W. Senaratne, C. Ober, and P. Neuzil, "Attogram Detection Using Nanoelectromechanical Oscillators", *Jour. of App. Phys.*, 2004, pp. 3694-3703.
- [2] N. V. Lavrik and P. G. Datskos, "Femtogram Mass Detection Using photothermally Actuated Nanomechanical Resonators", *App. Phys. Lett.*, April 2003, pp. 2697-2699.
- [3] K. L. Ekinci, Y. T. Yang, and M. L. Roukes, "Ultimate Limits to Inertial Mass Sensing Based Upon Nanoelectromechanical Systems", *Jour. of App. Phys.*, 2004, pp. 2682-2689.
- [4] S. Cherian and T. Thundat, "Determination of Adsorption-Induced Variation in the Spring Constant of a Microcantilever", *App. Phys. Lett.*, 2002, pp. 2219-2221.
- [5] R. Abdolvand and F. Ayazi, "Single-Mask Reduced-Gap Capacitive Micromachined Devices," *MEMS2005*, pp. 151-154.
- [6] A. Gupta, J. P. Denton, H. McNally, and R. Bashir, "Novel Fabrication Method for Surface Micromachined Thin Single-Crystal Silicon Cantilever Beams", *JMEMS*, Vol.12, No. 2, April 2003, pp. 185-192.
- [7] S. Pourkamali and F. Ayazi, "18 μm Thick High Frequency Capacitive HARPSS Resonators with Reduced Motional Resistance," Hilton Head, 2004, pp. 392-393.
- [8] S. Humad, R. Abdolvand, G.K. Ho, G. Piazza, and F. Ayazi, "High Frequency Micromechanical Piezo-On-Silicon Block Resonators," *IEDM2003*, pp. 957-960.